

Interactive comment on “Recent trends in climate variability at the local scale using 40 years of observations: the case of the Paris region of France” by J. Ringard et al.

Anonymous Referee #1

Received and published: 10 May 2019

Review of: Recent trends in climate variability at the local scale using 40 years of observations: the case of the Paris region France.

Summary: The analysis of variability of local scale uses temperature, moisture, and precipitation to evaluate 40 years of observations to attempt to identify thermodynamic versus dynamical changes in extreme events. The focus is on the summer season, with companion analysis of the other three seasons.

The goal of this manuscript is to determine the differences (if any) between thermodynamic and dynamic influences on extremes. I believe this is a good question and worth exploring this topic. Dynamical vs thermodynamical constraints are important

C1

considerations for the analysis of what drives extremes, especially within the context of climate change.

However, the authors do not use the correct definition of thermodynamics in their analysis. Temperature and humidity are analyzed independently, when there is well established literature demonstrating these variables are co-dependent. Temperature and humidity covary together, and non-linearly in extreme regimes. These can be readily calculated from Reynolds averaging (see eq. 13 from Buzan et al. 2015 for an example; shown below). From an analysis of the methods, I cannot determine if this was taken into account. The temperature and humidity plots are shown in isolation, and when they are mapped together (Fig. 14), they are based upon seasonal averages.

From the literature review, every major manuscript on temperature-moisture covariance from the past decade is missed (list of manuscripts below). To determine thermodynamically driven events, a pure thermodynamical variable should and a computed. Wet bulb temperatures/equivalent potential temperatures are linked to atmospheric convection, which demonstrated in theory (see Williams et al., 2009; figure below) and observation (Williams et al., 2017; example figure below). Wet bulb temperature maximums are directly tied to convection limits of the atmosphere. I recommend using Wet bulb temperature as they lead to clear thermodynamic events. However, there are other moist-temperature variables that could be utilized in the context of extremes such as evaporative cooling efficiencies (swamp cooler temperatures), heat stress metrics (e.g. Wet Bulb Globe Temperature which is temperature-radiation-moisture covariance). Overall, analyzing temperature and moisture independently fundamentally omits the total thermodynamical regime. I believe there are many more figures than are necessary for the analysis resulting from treating these state variables as independent.

Overall, I believe there are fundamental missing characteristics that are necessary to show thermodynamic vs dynamically driven changes in variability for the past 40 years. There is a lot of potential in this manuscript, and I am interested in evaluating a future manuscript that handles the full thermodynamics. Many of the same techniques

C2

evaluating maximums and correlating events would apply when using a pure moist thermodynamic variable.

Ex. 1) The observation stations (p. 4, line 8) shows warm-drier conditions Montsouris vs cooler-moist Trappes. The area between these stations is relatively small, and a metric such as wet bulb temperature or virtual temperature, I suspect, would show almost no difference between these stations. This is due to the moist-temperature covariance is fundamentally connected to equivalent potential temperatures, which are tied to the entropy state of the region (in other words, there are not significant differences in the total energy between the two stations).

2) Using wet bulb temperatures would remove the RH and q plots, and produce precipitation correlations between thermodynamics and dynamical driven processes. For example, figure 9 would consist of Tw and precipitation. Maximum wet bulb temperatures show clear pdf properties and have a clear non-gaussian shape (see Sherwood and Huber, 2010 figure 1E; posted below), thus the changes in Figure 13 should show clearer separations between the two time periods.

Supplemental: calculating moist-temperature values can be difficult. Choice of algorithms, especially in the context of extremes, can impact the results. I have attached code from the HumanIndexMod from the manuscript Buzan et al., 2015. The Davies-Jones wet bulb code is computationally fast and accurate to extreme conditions. The code is fortran designed to work with NCL fortran wrapper. T,P,Q are required; winds are optional.

References:

D Bolton. The computation of equivalent potential temperature. *Monthly Weather Review*, 108(7):1046–1053, 1980. J R Buzan, K Oleson, and M Huber. Implementation and comparison of a suite of heat stress metrics within the Community Land Model version 4.5. *Geosci. Model Dev.*, 8(2):151–170, 2015. Michael P Byrne and Paul A O’gorman. Link between land-ocean warming contrast and surface relative

C3

humidities in simulations with coupled climate models. *Geophysical Research Letters*, 40(19):5223–5227, October 2013.

Robert Davies-Jones. On Formulas for Equivalent Potential Temperature. *Monthly Weather Review*, 137(9):3137–3148, September 2009. Robert Davies-Jones. An Efficient and Accurate Method for Computing the Wet-Bulb Temperature along Pseudoadiabats. *Monthly Weather Review*, 136(7):2764–2785, July 2008. Noah Diffenbaugh, Jeremy Pal, Filippo Giorgi, and Xuejie Gao. Heat stress intensification in the Mediterranean climate change hotspot. *Geophysical Research Letters*, 34(11):L11706, 2007. E M Fischer, K W Oleson, and D M Lawrence. Contrasting urban and rural heat stress responses to climate change. *Geophysical Research Letters*, 39(3):1– 8, February 2012. Carlos D Hoyos and Peter J Webster. Evolution and modulation of tropical heating from the last glacial maximum through the twenty-first century. *Climate Dynamics*, 38(7-8):1501–1519, November 2011.

L S Kalkstein and J S Greene. An evaluation of climate/mortality relationships in large U.S. cities and the possible impacts of a climate change. *Environmental Health Perspectives*, 105(1):84, 1997. Robert L Korty, Kerry A Emanuel, Matthew Huber, and Ryan A Zamora. Tropical Cyclones Downscaled from Simulations with Very High Carbon Dioxide Levels. *J. Climate*, 30(2):649–667, January 2017.

Rahul Kumar, Vimal Mishra, Jonathan Buzan, Rohini Kumar, Drew Shindell, and Matthew Huber. Dominant control of agriculture and irrigation on urban heat island in india. *Scientific Reports*, 7(1):14054, 2017.

Mark G Lawrence. The Relationship between Relative Humidity and the Dew-point Temperature in Moist Air: A Simple Conversion and Applications. *Bulletin of the American Meteorological Society*, 86(2):225–233, February 2005.

Tom K R Matthews, Robert L Wilby, and Conor Murphy. Communicating the deadly consequences of global warming for human heat stress. *Proceedings of the National Academy of Sciences*, 114(15):3861–3866, April 2017.

C4

Brigitte Mueller and Sonia I Seneviratne. Hot days induced by precipitation deficits at the global scale. *Proceedings of the National Academy of Sciences of the United States of America*, 109(31):12398–12403, July 2012. — Steven C Sherwood and Matthew Huber. An adaptability limit to climate change due to heat stress. *Proceedings of the National Academy of Sciences*, 107(21):9552–9555, May 2010. — Katharine M Willett and Steven Sherwood. Exceedance of heat index thresholds for 15 regions under a warming climate using the wet-bulb globe temperature. *International journal of climatology*, 32(2):161–177, December 2010. — Ian N Williams, Raymond T Pierrehumbert, and Matthew Huber. Global warming, convective threshold and false thermostats. *Geophysical Research Letters*, 36(21):L21805, November 2009.

Ian N Williams and Raymond T Pierrehumbert. Observational evidence against strongly stabilizing tropical cloud feedbacks. *Geophysical Research Letters*, 44(3):1503–1510, 2017.

Ryan A Zamora, Robert L Korty, and Matthew Huber. Thermal Stratification in Simulations of Warm Climates: A Climatology Using Saturation Potential Vorticity. *J. Climate*, 29(14):5083–5102, July 2016.

Please also note the supplement to this comment:
<https://www.atmos-chem-phys-discuss.net/acp-2019-109/acp-2019-109-RC1-supplement.zip>

Interactive comment on *Atmos. Chem. Phys. Discuss.*, <https://doi.org/10.5194/acp-2019-109>, 2019.

C5

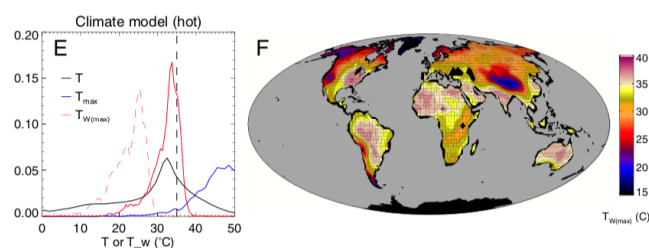


Fig. 1. (A) Histograms of 2-meter T (Black), T_{\max} (Blue), and $T_{W(\max)}$ (Red) on land from 60S–60N during the last decade (1999–2008). “Max” histograms are annual maxima accumulated over location and year, while the T histogram is accumulated over location and reanalysis time. Data are from the ERA-Interim reanalysis 4xdaily product (similar results are found for the 50m level from the NCEP reanalysis, see *SI Text*). (B) Map of $T_{W(\max)}$. (C and D) Same as A and B but from a slab-ocean version of the CAM3 climate model that produces global-mean surface temperature close to modern values. (E and F) Same as C and D but from a high- CO_2 model run that produces a global-mean T 12 °C warmer; accounting for GCM bias, the $T_{W(\max)}$ distributions are roughly what would be expected with 10 °C of global-mean warming relative to the last decade (see text). Dashed line in E is $T_{W(\max)}$ reproduced from C. White land areas in F exceed 35 °C.

Fig. 1. Sherwood and Huber figure

C6

$$\begin{aligned}
\overline{HI} = & a + \overline{bT} + \overline{cRH} + \overline{dTRH} + \overline{eT^2} + \overline{fRH^2} \\
& + \overline{gT^2RH} + \overline{hTRH^2} + \overline{iT^2RH^2} \\
& + \left[\overline{dRH'T'} + \overline{eT'^2} + \overline{fRH'^2} + \overline{gT'^2RH'} \right. \\
& \left. + \overline{hT'RH'^2} + \overline{iT'^2RH'^2} \right], \tag{13}
\end{aligned}$$

where $a, b, c, d, e, f, g, h,$ and i are constants in the polynomial. RH and T are relative humidity and temperature, respectively. We are not concerned with the terms outside the brackets, as they are the means. The terms within the bracket are representative of turbulent effects on the heat index, which we are discussing. It is these turbulent states

Fig. 2. Buzan2015_Eq.13

C7

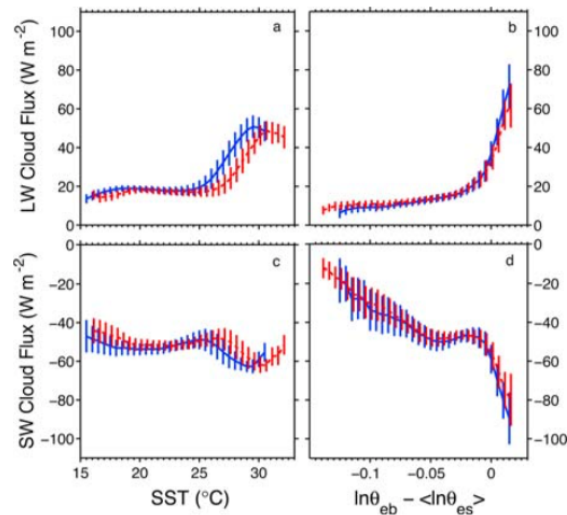


Figure 1. TOA cloud LW flux as a function of (a) SST and (b) s_{diff} ; TOA cloud SW flux as a function of (c) SST and (d) s_{diff} ; Solid blue and dashed red lines correspond to the ensemble median over years 0–20 and 60–80, respectively, from 15 IPCC AR4 coupled ocean-atmosphere models for the 1% per year scenario. Vertical lines indicate the interquartile range.

Fig. 3. Williams_2009_Moist_Convection_Limits_Theory

C8

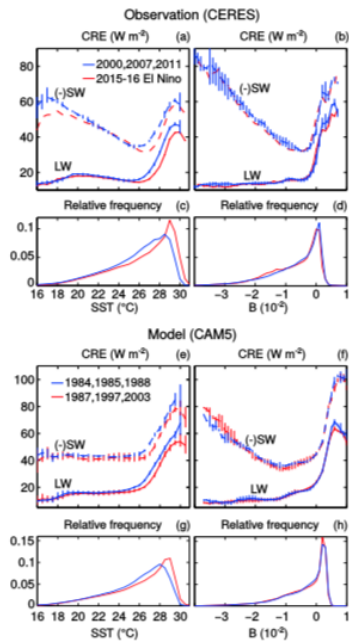


Figure 2. Effects of tropics-wide SST variability on observed and modeled CRE, shown as functions of local SST (Figures 2a, 2c, 2e, and 2g) and B (Figures 2b, 2d, 2f, and 2h). (a) The SST distributions of (minus) shortwave (dashed lines) and longwave (solid lines) CRE shift almost uniformly to warmer SSTs during the 2015–2016 El Niño relative to the three coldest years observed. (b) The buoyancy distribution of CRE is approximately invariant with warming. (c) Relative frequency distributions show that warming is approximately uniform across SST. (d) Warming results in little change to the relative frequency distribution of buoyancy. (e–h) As in Figures 2a–2d but for CAM5-AMIP simulations, for the three warmest and coldest simulated years. Error bars indicate the range over all three years.

Fig. 4. Williams_2017_Moist_Convection_Limits_Observation